

Lisa S. Darby and Robert M. Banta

*National Oceanic and Atmospheric Administration, Environmental Technology Laboratory, Boulder, Colorado  
and*

Roger A. Pielke, Sr.

*Colorado State University, Department of Atmospheric Science, Fort Collins, Colorado*

## 1. INTRODUCTION

A National Oceanic and Atmospheric Administration/Environmental Technology Laboratory (NOAA/ETL) Doppler lidar measured the diurnal life cycle of the land and sea-breeze system along the California coast under various synoptic conditions during the Land and Sea Breeze Experiment (LASBEX) in September 1987. The lidar was stationed at Moss Landing, 1.5 km east of the shore of Monterey Bay (Fig. 1), measuring winds on 12 days. On days with offshore synoptic flow, the transition to onshore flow (the sea breeze) was a distinct process easily detected by lidar. Fine-scale lidar measurements showed the reversal from offshore to onshore flow near the coast, and its gradual vertical and horizontal expansion. Lidar scans taken along an east/west cross-shore line, horizon-to-horizon, on days with ambient offshore flow, showed a dual structure to the sea-breeze flow. Initially, a shallow (<500 m) sea breeze formed which later became embedded in a weaker onshore flow that was ~1 km deep. Eventually these two flows blended together to form a mature sea breeze at least 1 km deep. Detailed background information on this study can be found in Intrieri et al. (1990), Banta et al. (1993), and Banta (1995).

Regional Atmospheric Modeling System (RAMS) two-dimensional simulations successfully simulated this dual

structure of the sea-breeze flow when both the coastal mountain range just east of Monterey Bay and the Sierra Nevada range, peaking 300 km east of the shore, were included in the domain. Various sensitivity simulations were conducted to isolate the roles played by the land/water contrast, the coastal mountain range, and the Sierra Nevada range in the vertical structure of the sea-breeze flow at Monterey Bay. A factor separation method was employed to further isolate the contributions of the terrain and land/water contrast to the vertical structure of the modeled  $u$ -component of the wind.

## 2. LIDAR MEASUREMENTS

On 16 September 1987, the Doppler lidar measured the early morning offshore winds, the transition to the sea-breeze (onshore) flow, the maturation of the sea breeze, and the evening transition to offshore flow. Throughout the day, the lidar regularly scanned from horizon-to-horizon, along an east-west line perpendicular to the coast. The data in these scans were converted from polar to Cartesian coordinates, and radial velocities were divided by the cosine of the elevation angle of the lidar beam to retrieve the component of the wind parallel to the plane of the scan, in this case the  $u$ -component of the wind. As explained in detail in Banta et al. (1993) and

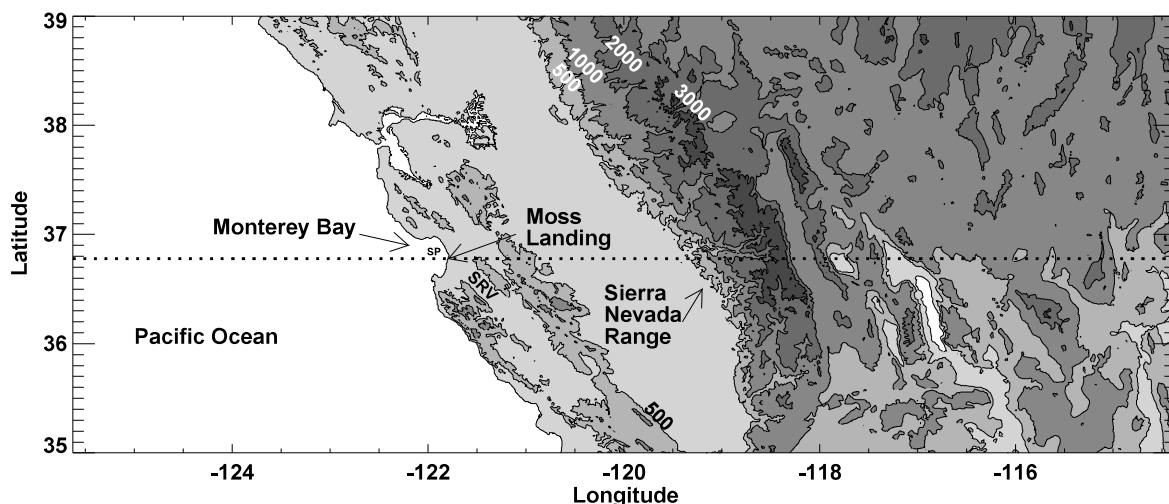


Fig. 1 Terrain map showing the location of LASBEX (most instrumentation deployed near Moss Landing) and the modeling domain, indicated by the dotted horizontal line at the same latitude as the lidar deployment. Contours are every 1000 m except for a 500 m contour added for more detail between the Sierra Nevada Range and the coast. The approximate location of the R/V Silver Prince is indicated by SP, the Salinas River Valley by SRV.

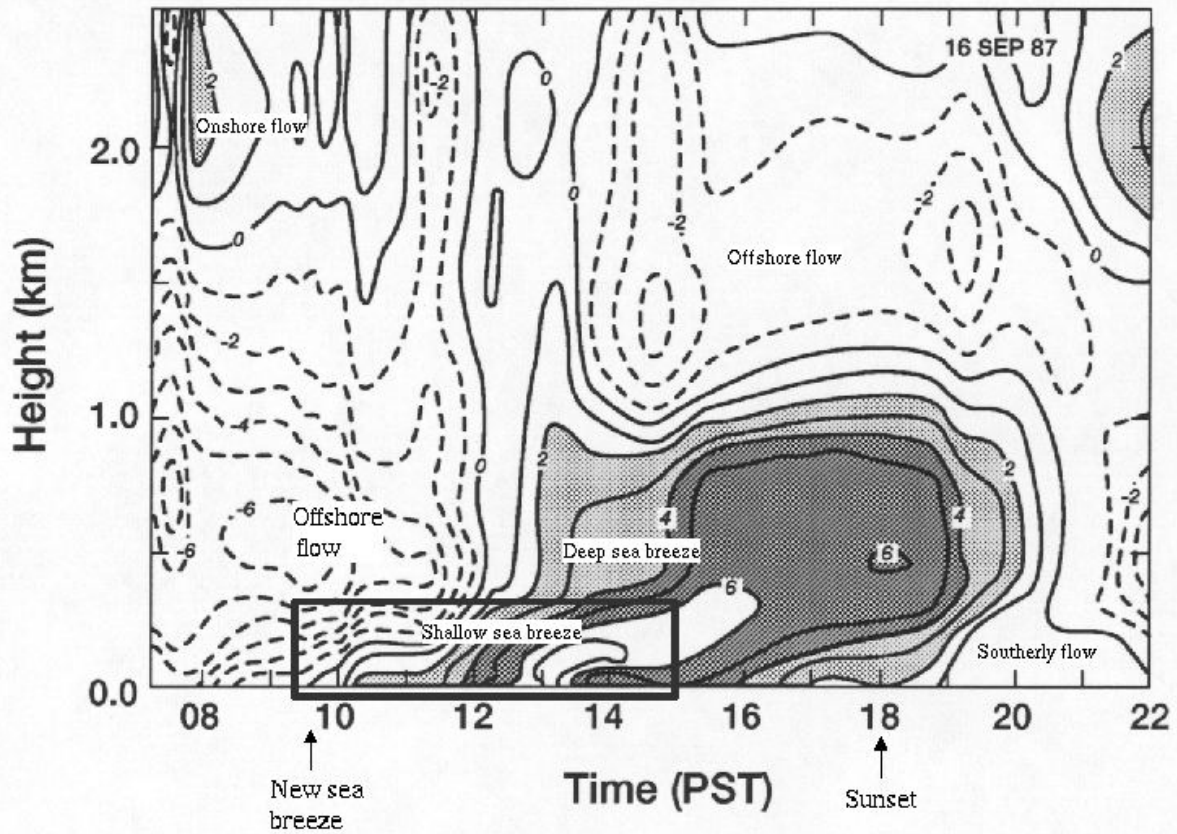


Fig. 2 Time-height series of vertical profiles of the  $u$ -component of the wind as measured by the ETL Doppler lidar (from Banta et al. 1993). Dashed lines represent flow from the east (offshore), solid lines flow from the west (onshore). Westerly flow  $2\text{--}4\text{ m s}^{-1}$  has light shading, flow from  $4\text{ to }6\text{ m s}^{-1}$  has heavier shading.

Banta (1995), from these data, profiles of the wind just offshore were derived and then combined into a time-height series, shown in Fig. 2. Key features seen in this figure include a shallow, stronger sea breeze imbedded in a weaker, deeper onshore flow, and the blending of these two-scales of onshore flow into a deep, mature sea breeze.

### 3. MESOSCALE 2-D MODELING

RAMS simulations were executed two times for the 5 different terrain configurations shown in Fig. 3. The first set of five simulations had water in the western portion of the domain (to the left of  $x = 0$ ). The second set of five simulations had no water, only short grass, in the domain. The domain was much larger than what is shown in Fig. 3, with the horizontal extent of the domain indicated by the dotted line in Fig. 1. The vertical grid spacing was 25 m from the ground to 1.2 km AGL, and then gradually expanded, never exceeding 500 m, extending to 15 km AGL. The horizontal grid spacing was 2 km.

From each simulation, a vertical profile of the  $u$ -component of the wind was extracted from the shoreline every half-hour of the simulation. These profiles were plotted in the same manner as the lidar time-height series for comparisons with the lidar data. Except for the

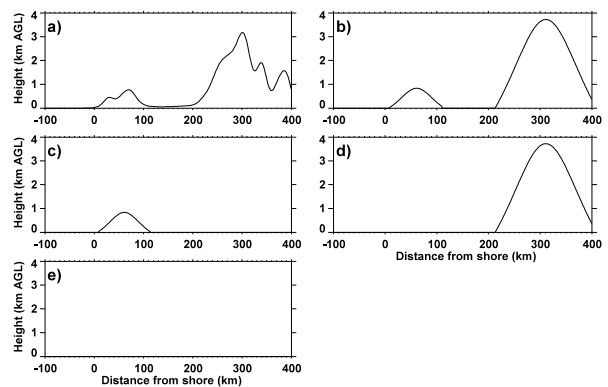


Fig. 3 The terrain profiles used in the model sensitivity studies. Only the part of the domain immediately surrounding the terrain is shown. The terrain is referred to in the text as: (a) Dual-mountain (smoothed); (b) dual-mountain; (c) coastal mountain; (d) inland mountain; and (e) flat.

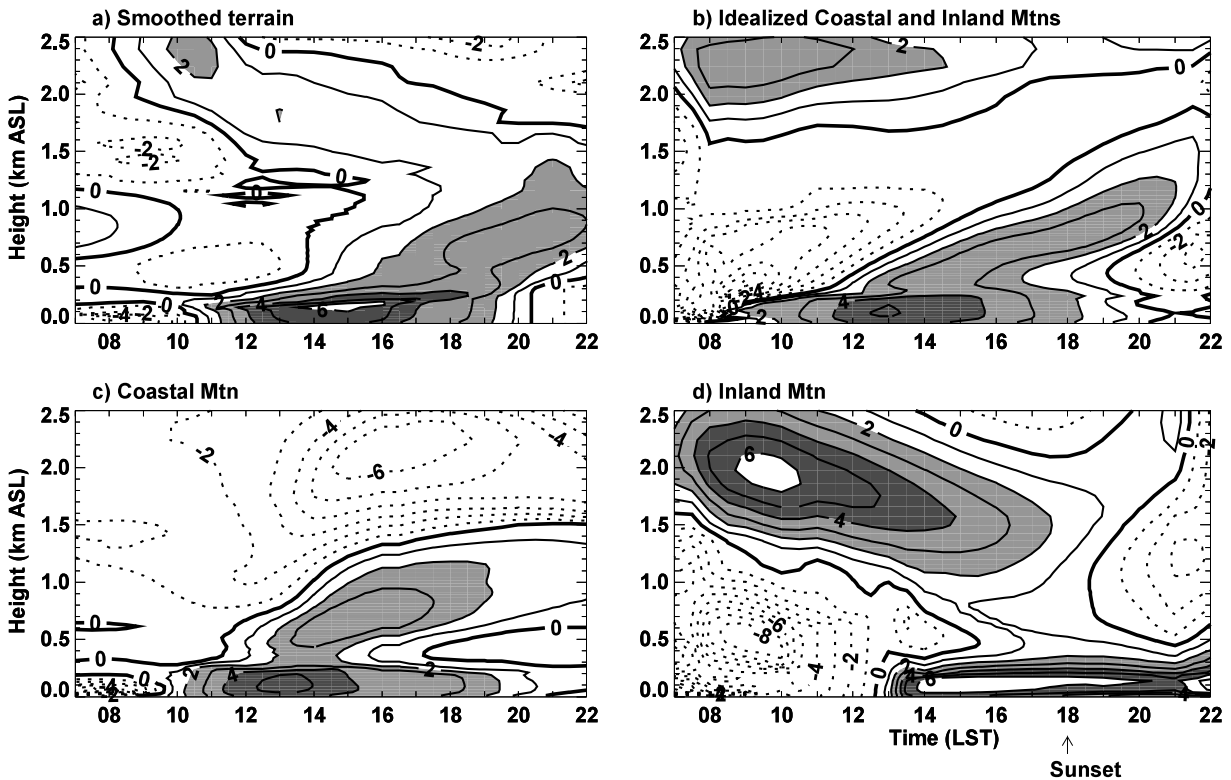


Fig. 4 Time-height series of the  $u$ -component of the wind (in  $m\ s^{-1}$ ) extracted from the shore in simulations with water in the western portion of the domain. Profiles were extracted on the hour and half-hour from 0700 to 2200 LST. Solid (positive) contours indicate westerly flow. Dashed contours indicate easterly flow. Westerly flow  $2-4\ m\ s^{-1}$  has medium shading and flow  $4-6\ m\ s^{-1}$  has dark shading. (a) Dual-mountain (smoothed); (b) dual-mountain; (c) coastal mountain; and (d) inland mountain.

simulations without elevated terrain, Fig. 4 shows the results from the simulations with water in the domain, and Fig. 5 shows the results from the simulations without water in the domain.

#### 4. COMPARISON OF MODEL RESULTS TO LIDAR MEASUREMENTS

The model results that most closely resembled the lidar measurements were the two simulations that included the land/water contrast and both a coastal mountain range and inland mountain range (Figures 4a and 4b). Each of these simulations had a shallow sea breeze that existed for a couple of hours before a weaker, deeper onshore flow developed, as seen in the lidar data. In the morning, both of these simulations also showed weak westerly flow above 2 km, as in the lidar measurements.

Removing the inland mountain range (Fig. 4c) did not remove the dual structure to the onshore flow. However, all westerly flow above 2 km was eliminated. This implies that the coastal mountain was associated with the dual structure of the sea-breeze flow, and the inland mountain affected the flow above the sea-breeze layer at the shore, even though its peak was  $\sim 300$  km inland. Removing the coastal mountain and leaving the inland mountain in the domain (Fig. 4d) greatly affected the vertical structure

of the flow at the shoreline. Only a shallow sea breeze, stronger than in the dual-mountain cases, developed under these conditions. In this 2-D setting, the inland mountain generated strong downslope flow at night, with a strong compensating westerly return flow that did not decay until the afternoon, showing up in the time-height series as the strong westerly flow above 1 km AGL. Without terrain in the domain, the strongest sea breeze of the simulations formed, with a maximum speed of  $8\ m\ s^{-1}$ , a depth of  $\sim 600$  m, and a weak return flow (not shown).

In the two simulations with both mountains in the domain, but no land/water contrast, (Figures 5a and 5b) the wind flow above 2.0 km AGL was very similar to the winds seen in the simulations with water (Figures 4a and 4b) implying that the land/water contrast did not have a dominating effect above 2.0 km. The westerly upslope flows associated with the coastal mountain were weak and deep, with a fairly sudden onset. The comparison among the simulations with and without the land/water contrast and with and without the coastal mountain imply that the coastal mountain slope flow enhanced the depth of the sea-breeze flow.

#### 5. FACTOR SEPARATION

The above figures illustrate the effects of different

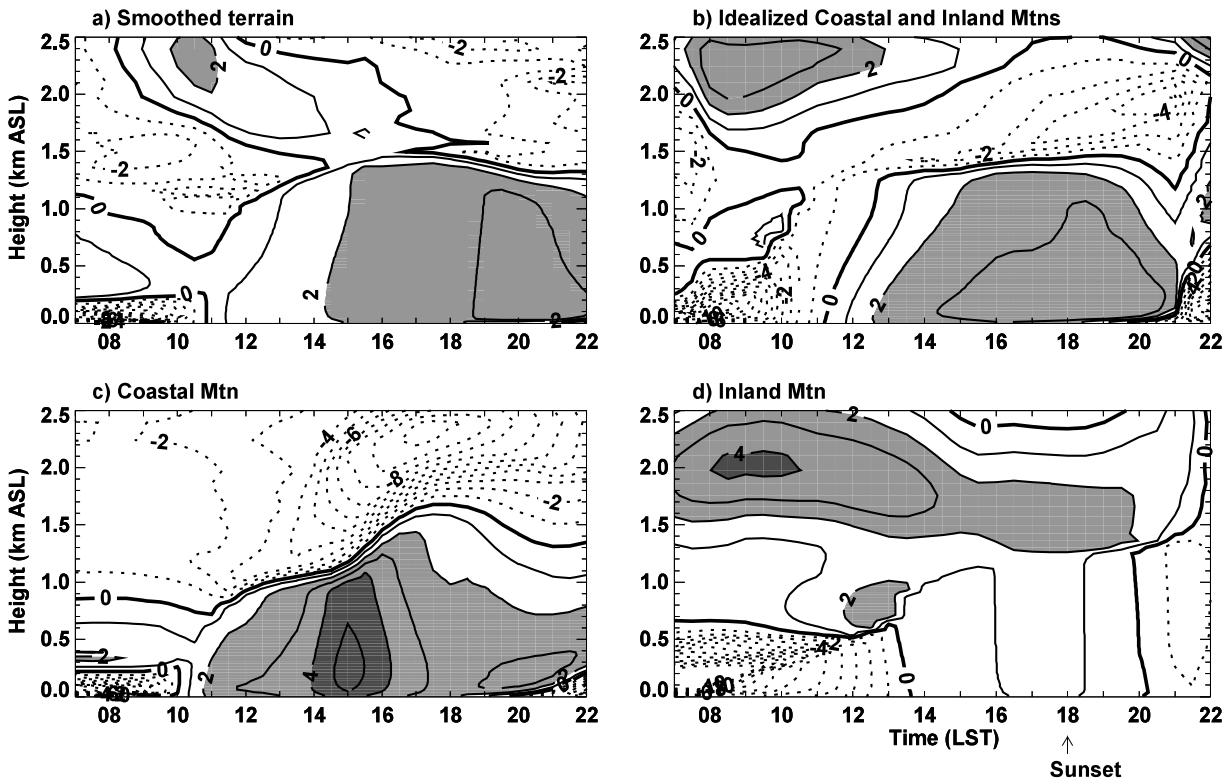


Fig. 5 As in Fig. 4, except for simulations with short grass rather than water in the western portion of the domain.

topography and land surface features on the sea breeze development. An interesting question is whether combinations of surface features interact in such a way to enhance or decrease the onshore flow. To answer these questions, we employ the factor separation method of Stein and Alpert (1993). Their method stresses that investigators need to look at not only the differences between simulations with and without the factors under investigation (e.g., terrain and the land/water contrast), but that the interaction of factors under consideration is also important. Based on the equations presented in Stein and Alpert (1993), and the simulations using the terrain shown in Figs. 3b-3d (with and without water in the domain), the  $u$ -component of the wind as the result of the interaction of flows produced by 2 different factor pairs and a triple interaction are shown in Fig. 6.

To fully understand the plots illustrating the wind flow as a result of the interaction of flows produced by the factors, there are three things to look for in Fig. 6: 1) Where are the values equal to zero? The interaction of factors has no effect on the  $u$ -component of the wind, the field of interest, where the values plotted are equal to zero; 2) Where are the regions of values of greatest magnitude plotted? These are the places where the interaction has the most effect; and 3) What is the sign of these regions of greatest magnitude relative to the simulation including all factors under consideration (refer to Fig. 4b)? If the sign is the same as in the corresponding region of the model simulation with all factors present, then the interaction of the factors enhanced the modeled

flow; if the sign is opposite, then the interaction of factors opposed, i.e., weakened, the modeled flow.

The results for the interaction of slope flows generated by both the coastal and inland mountains (Fig. 6a) revealed that in the early morning hours the onshore flow was strongly enhanced below 300 m, with only a slight enhancement after 1300 LST, which is when the modeled sea-breeze flow began to weaken (Fig. 4b). This maximum in the early morning enhancement corresponded to the onset of the shallow sea breeze seen in the model results (Fig. 4b) and the lidar results (Fig. 2). Based on this method and this factor pair, having both mountain ranges in the domain enhanced the shallow sea-breeze flow throughout the day. However, this interaction did not enhance the deeper sea breeze, as evidenced by the enhancement of easterly flow (dashed lines) seen between 500 m and 1500 m. Looking at the winds resulting from the interaction of flows generated by all terrain and the land/water contrast (Fig. 6b), again, there was some enhancement of onshore flow in the early morning, although not as strong as in the previous factor pair. After 1200 LST the interaction began to oppose the afternoon offshore flow in a layer that steadily increased in depth with time. This implies that while the slope flows acted to enhance the sea-breeze flow in the initial stages in the morning, the terrain also acted as a barrier, and worked to oppose the sea breeze, particularly after sunset when downslope flows began to form. This interaction weakly enhanced the deeper sea breeze, especially later in the day, as seen in the westerly flow (solid lines) above 500

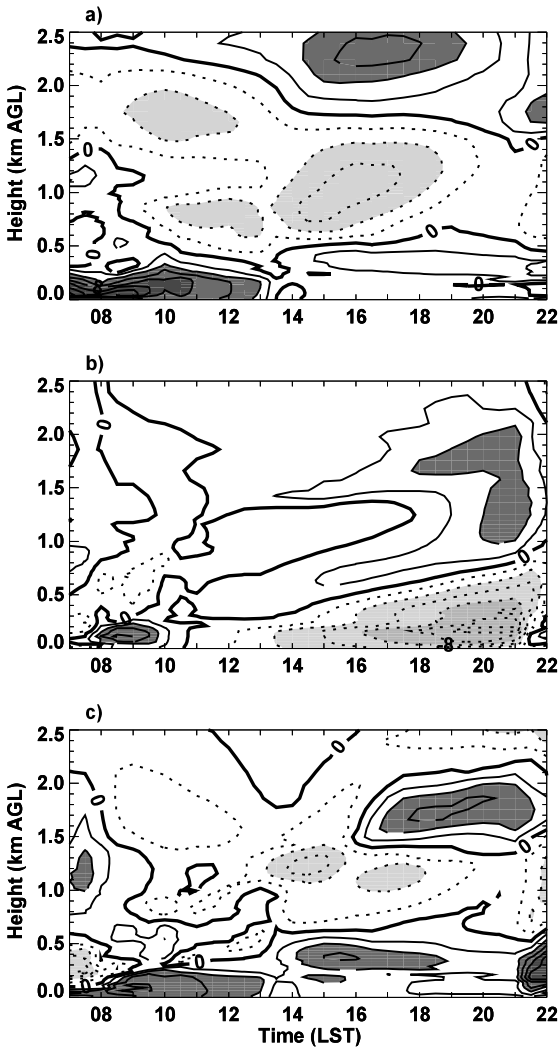


Fig. 6 Time-height cross section of the wind field resulting from the interaction of two factor pairs and a triple interaction. Solid contours represent westerly flow, dashed contours represent easterly flow. Dark gray shades (westerly flow greater than  $4 \text{ m s}^{-1}$ ) show where westerly flow was enhanced by the interactions. Light gray (easterly flow greater than  $4 \text{ m s}^{-1}$ ) indicate where easterly flow was enhanced by the interactions. (a) Flow due to the interaction of mountain induced flows. (b) Flow due to the interaction of the slope flows and the land/sea breeze. (c) Flow due to the triple interaction of the coastal mountain flows, inland mountain flows, and the land/sea breeze.

m to 1000 m after 1200 LST. There was very little effect above 1 km before 1800 LST, fitting in with the small difference seen above 1 km between the simulations with and without the land/water contrast. The results from the interaction of flows due to the coastal mountain, inland

mountain, and the land/water contrast (Fig. 6c) show that early in the morning the onshore flow was enhanced in the lowest 300 m, and after 1400 LST the onshore flow was enhanced in a slightly elevated layer, corresponding with the formation of deeper onshore flow seen in Fig. 4b.

## 6. CONCLUDING REMARKS

To model the sea breeze at Monterey Bay in 2 dimensions requires that both the coastal and inland mountain ranges be included in the domain for the most realistic results, based on comparisons with lidar measurements perpendicular to the shore. Simulations and the factor separation results suggest that major features of the sea-breeze flow result from 2-D topographic and land-surface features. Therefore, 2-D modeling is an appropriate avenue for investigating the sea breeze at Monterey Bay. This is not to imply, however, that the sea breeze at Monterey Bay is solely a 2-dimensional problem. Because of the terrain surrounding the bay, and the shape of the bay itself, the wind flow in this region is highly 3-dimensional. The combination of high-resolution lidar measurements of the vertical structure of the onshore flow with high-vertical-resolution model simulations is an excellent starting point for understanding the physical processes associated with the sea breeze at Monterey Bay.

## REFERENCES

- Banta, R.M., 1995: Sea breezes shallow and deep on the California coast. *Mon. Wea. Rev.*, **123**, 3614-3622.
- \_\_\_\_\_, L. D. Olivier, and D. H. Levinson, 1993: Evolution of the Monterey Bay sea-breeze layer as observed by pulsed Doppler lidar. *J. Atmos. Sci.*, **50**, 3959-3982.
- Intrieri, J.M., C.G. Little, W.J. Shaw, R.M. Banta, P.A. Durkee, and R.M. Hardesty, 1990: The Land/Sea Breeze Experiment (LASBEX). *Bull. Amer. Meteor. Soc.*, **71**, 656-664.
- Stein, U., and P. Alpert, 1993: Factor separation in numerical simulations. *J. Atmos. Sci.*, **50**, 2107-2115.

<http://www.etl.noaa.gov>

<http://www.atmos.colostate.edu>

Corresponding author address: Lisa S. Darby, NOAA/ETL, R/E/ET2, 325 Broadway, Boulder, CO, 80305; e-mail: lisa.darby@noaa.gov.